Available online at www.sciencedirect.com
SCIENCE DIRECT
ELSEVIER
Journal of Crystal Growth 268 (2004) 364–368
JOURNAL OF CRYSTAL GROWTH
www.elsevier.com/locate/jcrysgro

InGaAs/GaAs quantum well circular ring lasers fabricated by laser direct writing and pulsed anodic oxidation

C.Y. Liu*, Shu Yuan

School of Materials Engineering, Nanyang Technological University, Singapore, 639798, Singapore

Abstract

We report the fabrication of $In_{0.22}Ga_{0.78}As/GaAs$ single quantum well circular ring lasers with an integrated output stripe (two cleaved facets) by using laser direct writing lithography, wet chemical etching and subsequent pulsed anodic oxidation. The laser works under continuous wave operation at room temperature with a low threshold current density of 80 A/cm^2, a slope efficiency of 0.26/W/A per facet.
© 2004 Elsevier B.V. All rights reserved.

PACS: 81.40.Wx; 85.30.De; 68.47.Gh; 42.55.Px

Keywords: A1. Characterization; A1. Etching; B1. Oxides; B3. Laser diodes

1. Introduction

InGaAs/GaAs strained-layer quantum well (QW) laser diodes extend the emission wavelength from 0.9 to 1.1 μm, which is an unobtainable range by previous AlGaAs/GaAs and InGaAsP/InP system [1,2]. The 980 nm InGaAs/GaAs QW lasers are particularly attractive for the pumping source of erbium-doped fiber amplifiers (EDFAs) [3,4] because the 980 nm pumping system provides not only high gain [3–5] but also low-noise amplification [6].

Since their first demonstration [7], semiconductor ring lasers (SRLs) have received much attention owing to their applications in photonic integrated circuits (PIC). They are promising candidates for wavelength filtering, unidirectional traveling wave operation and multiplexing/demultiplexing applications [8–12]. Several examples of fabrication of SRLs with different cavity geometries have been reported, such as circular [13,14], racetrack [15,16], square [11,17], and triangular [18].

In the fabrication of SRLs, in order to be practical, ring laser resonators must provide strong lateral guiding. Currently, most SRLs are fabricated using patterned reactive ion etching (RIE) extending below the QW active region, thus forming sidewalls that provide the large index step necessary for guiding the optical mode around "tight" bends. A disadvantage observed in this fabrication method is accelerated degradation due to atmospheric exposure of the active region at the sidewall semiconductor/air interface. An insulating layer will be helpful to overcome

*Corresponding author.
E-mail address: p149365285@ntu.edu.sg (C.Y. Liu).

0022-0248/$ - see front matter © 2004 Elsevier B.V. All rights reserved.
doi:10.1016/j.jcrysgro.2004.04.055

above-mentioned problem to some extent. However, the conventional SiO_2 deposited by plasma enhance chemical vapor deposition (PECVD) is not suitable for this purpose, for it may have high chance to damage the exposed active region during the deposition. Another approach is to use the native oxide formed by wet thermal oxidation [19] or pulsed anodic oxidation (PAO) [20,21]. However, wet thermal oxidation is also not the perfect choice for the fabrication of SRLs. For this method was limited to high Al content, and what's more, the oxidation rate of $Al_xGa_{1-x}As$ is highly dependent on the Al composition. In order to achieve "deep oxidation", which is important for large lateral index contrast mentioned above, silicon impurity-induced layer disordering (IILD) process has to be performed to intermix high and low-x $Al_xGa_{1-x}As$ in preparation for oxidation [19]. Without IILD step, higher-x $Al_xGa_{1-x}As$ confinement layers typical oxidized laterally beneath the mask. And it will pinch off the current path. Thus, a simple oxidation process that is suitable for "deep oxidation" would greatly simplify the fabrication process of circular ring-geometry lasers. PAO has been demonstrated to be very useful as current-blocking layer in the semiconductor laser fabrication [20,21]. Furthermore, it is also a self-aligned isolation method, a kind of planarization; thus, it can improve the sidewall quality and reduce the damage during the wet etching.

In this work, we report the fabrication of $In_{0.22}Ga_{0.78}As/GaAs$ single quantum well (SQW) circular ring lasers with an integrated output stripe (two cleaved facets) by using laser direct writing lithography (DWL), wet chemical etching and subsequent PAO with high performance for the first time, to the best of our knowledge.

2. Experimental procedure

$In_{0.22}Ga_{0.78}As/GaAs$ graded index separated confinement heterostructure (GRINSCH) SQW laser structure used in this study was grown by low-pressure metal organic chemical vapor deposition (MOCVD). The complete laser structure is listed Table 1.

Table 1
$In_{0.22}Ga_{0.78}As/GaAs$ 980 nm laser structure

Layer	Al comp.	Thickness (nm)	Doping (cm^{-3})
GaAs	0	200	~1e20 (p)Zn
AlGaAs→GaAs	0.6 to 0	150	~1e18(p)Zn
AlGaAs	0.6	1000	~1e18(p)Zn
AlGaAs	0.6	100	i
GaAs→AlGaAs	0 to 0.6	150	i
GaAs	0	12	i
InGaAs (single QW)	In (0.2)	7.3	i
GaAs	0	12	i
AlGaAs→GaAs	0.6 to 0	150	i
AlGaAs	0.6	1000	~1e18(n)Si
GaAs→AlGaAs	0 to 0.6	150	~1e18(n)Si
GaAs buffer	0	250	~1e18(n)Si
n+(100) GaAs substrate	0	a.u.	~1e18(n)Si

The major fabrication steps of circular ring laser are as following: the wafer was cleaved into desired size ($7\times7\,mm^2$) first, and then cleaned carefully. To pattern on the wafer for mesa etching, a layer of positive photoresist EPG 510 is spin-coated on the sample at room temperature at 4000 rpm for 35 s, followed with a soft bake on 90°C hot plate for 90 s. A circular ring pattern was generated with the DWL and developing followed by the hard bake on 110°C hotplate for 90 s, with an outer radius of 250 μm, an inner radius of 200 μm, respectively, the contact ridge width of 50 μm for both the ring and the stripe. DWL lithography means writing with a finely focused laser beam directly on a photoresist-coated substrate to get the desired pattern, i.e., a maskless lithography technique. The laser used in this work is a 442-nm HeCd laser, works in the CW operation mode at room temperature with the output power of 180 mW. The spot diameter of the laser beam is 0.8 μm.

The mesa was formed by wet chemical etching with $H_3PO_4/H_2O_2/H_2O$ (1:1:5) solution. During the etching, photoresist serves as the etching mask, so only the part without photoresist coating was etched. After etching, the PAO process is performed to get a layer of native oxide on the etched surface. Fig. 1 shows the schematic of the experimental setup for PAO used in this work. It

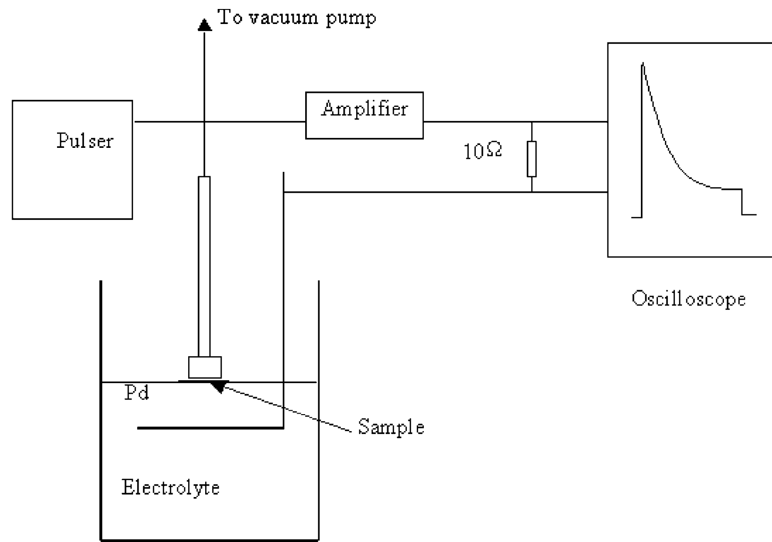

Fig. 1. Schematic of experimental set up for pulsed anodic oxide growth.

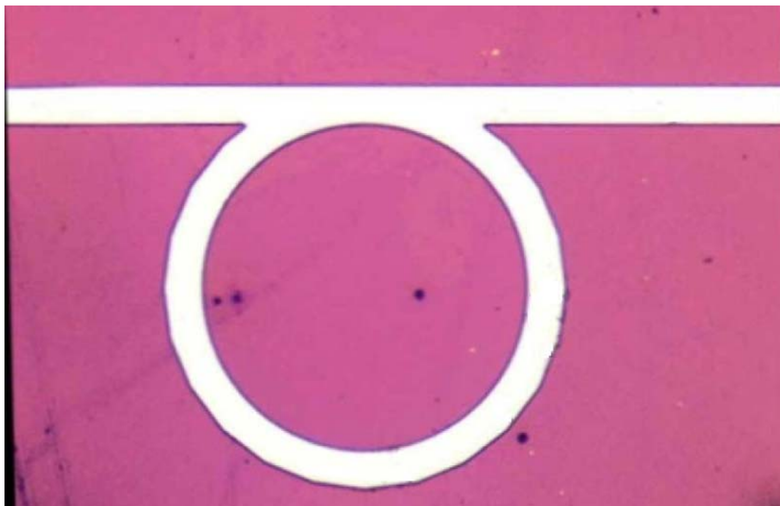

Fig. 2. Optical microscopy image of the top view of a circular ring pattern with a stripe coupler. The dark part is anodic oxide formed by using pulsed anodic oxidation.

consists of the following components: a cathode, a pulsed voltage source, a 10 Ω resistor, a power amplifier, a vacuum pump with the metal vacuum holder, an oscilloscope as well as the electrolyte. The electrolyte was a mixture of ethylene glycol, de-ionized water (D. I. Water) and phosphoric acid in the ratio of 40:20:1, respectively, with a typical PH value around 6.2. The PH value of the solution will not be adjusted during oxidation. The cathode, generally of platinum or an other noble metal, is immersed in the electrolyte and connected to the pulse voltage source through the resistor. The semiconductor samples to be oxidized are immersed in the electrolyte, and electrically connected to metal holder, which serves as an anode, by vacuum suction. The samples to be

oxidized are in series with the resistor. The voltage across the resistor is monitored by an oscilloscope to observe the oxidation process. For typical oxide growth, the voltage pulse width is 700 μs, the frequency is 144 Hz, pulse voltage ranges from 60 to 80 V and typical oxidation time is 4 min for an oxide with the thickness in the range of ~200 to 220 nm. During the oxidation, photoresist serves as the mask, so only the part without photoresist coating was oxidized. The oxidation is performed at room temperature. After pulsed anodic oxidation, the photoresist stripes remained on the wafer is removed with acetone and rinsed with D. I. water and then dried by using nitrogen.

Ti/Au (50/200 nm) is e-beam evaporated on the mesa top as the p-contact. After the sample is lapped down to below 100 μm, AuGe/Ni/Au

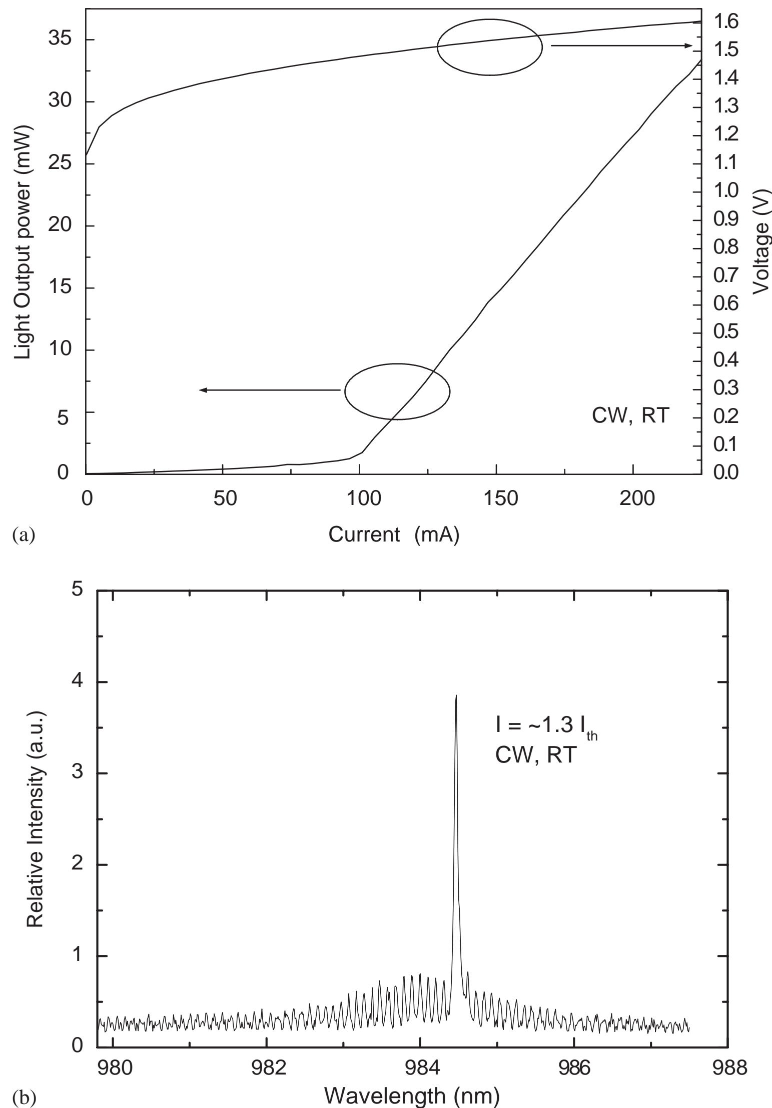

Fig. 3. (a) CW light output power–current–Voltage (*L–I–V*) characteristics of $In_{0.22}Ga_{0.78}As/GaAs$ ring laser tested at room temperature, ridge width $W = 50\,\mu m$, laser cavity length $L = 1200\,\mu m$, radius of the outer ring $R_{outer} = 250\,\mu m$, radius of the inner ring $R_{Inner} = 200\,\mu m$. (b) The emission spectrum taken at $I = \sim 1.3 \times I$th at room temperature.

(150 nm/15 nm/150 nm) is e-beam evaporated on the bottom of the sample as the n-contact. And then the sample is alloyed at 410°C for 1 min. After finishing all the fabrication processes, the wafer was cleaved into single chips for testing. The ring laser has been tested without facet coating and intentional heatsink at room temperature under CW operation.

3. Results and conclusions

Fig. 2 shows the optical microscopy image of the top view of a circular ring pattern with an output stripe coupler fabricated by using DWL followed by conventional wet etching as well as subsequent PAO. Circular ring lasers have an outer radius of 250 μm, and an inner radius of 200 μm, thus the contact ridge width is 50 μm for both the ring and the stripe. The dark part is anodic oxide formed by using PAO, which acts as the isolation layer for the current injection.

Fig. 3(a) shows a typical light output power–current–voltage characteristics (*L–I–V*) of an $In_{0.22}Ga_{0.78}As/GaAs$ circular ring laser, with the cavity length of 1200 μm, ridge width $W = 50\,\mu m$, radius of the outer ring $R_{outer} = 250\,\mu m$, and radius of the inner ring $R_{inner} = 200\,\mu m$. Fig. 3(b) shows the corresponding laser emission spectrum measured at an inject current of $\sim 1.3 \times I$th. From both figures, it can be seen that the laser works under CW operation at room temperature with a very low threshold current density of 80 A/cm^2, a slope efficiency of 0.26 W/A per facet at 980 nm emission wavelength ranges, which shows high performance of the circular ring laser.

To the best of our knowledge, this is the first time demonstration of circular ring laser fabrication with DWL and PAO for deep oxidation. It can be seen that DWL provides great flexibility in the pattern design and PAO process is a convenient, reliable, and cost effective method in the laser diode fabrication. With this method, the previously complicated and crucial process has been greatly simplified, to a more manufacturable and thus, commercially viable level, and may stimulate further advances in optoelectronics devices and photonic integrated circuit (PIC).

Acknowledgements

The authors thank Professor C. Jagadish for providing $In_{0.22}Ga_{0.78}As/GaAs$ SQW laser structure sample and Dr. Qu Yi for valuable discussions and careful reading of the manuscript.

References

[1] J.Y. Marzin, M.N. Charasse, B. Sermage, Phys. Rev. B 31 (1985) 8298.
[2] T.G. Andersson, Z.G. Chen, V.D. Kulakovskii, A. Uddin, J.T. Vallin, Phys. Rev. B 37 (1988) 4032.
[3] K. Suzuki, Y. Kimura, M. Nakazawa, Appl. Phys. Lett. 55 (1989) 2573.
[4] R.I. Laming, M.C. Parries, P.R. Morkel, L. Reekie, D.N. Payne, P.L. Scrivener, F. Fontana, A. Righetti, Electron. Lett. 25 (1989) 12.
[5] R.B. Laier, CTTE lab incorporation, laser diode technology and applications IV, SPIE 1219 (1992) 268.
[6] A. Kasukawa, T. Mukaihara, T. Yamaguchi, J. Kikawa, Fukurawa Electric 19 (2000) 23.
[7] A.S. Liao, S. Wang, Appl. Phys. Lett. 36 (1980) 801.
[8] J.P. Hohimer, G.A. Vawter, Appl. Phys. Lett. 63 (1993) 1598.
[9] J.P. Hohimer, G.A. Vawter, Unidirectional semiconductor ring lasers with racetrack cavities, Appl. Phys. Lett. 63 (1993) 2457.
[10] J.J. Liang, S.T. Lau, M.H. Leary, J.M. Ballantyne, Appl. Phys. Lett. 70 (1997) 1192.
[11] S. Oku, M. Okayas, M. Ikeda, IEEE Photon Technol. Lett. 3 (1991) 588.
[12] S. Oku, M. Okayasu, M. Ikeda, IEEE Photon Technol. Lett. 3 (1991) 1066.
[13] T.F. Krauss, R.M. De La Rue, P.J.R. Laybourn, B. Vogele, C.R. Stanley, IEEE J. Select. Top. Quantum Electron. 1 (1995) 757.
[14] J.P. Hohimer, D.C. Craft, G.R. Hadley, G.A. Vawter, Electron. Lett. 28 (1992) 374.
[15] G. Griffel, J.H. Abeles, R.J. Menna, A.M. Braun, J.C. Connolly, M. King, IEEE Photon Technol. Lett. 12 (2000) 146.
[16] J.P. Hohimer, G.A. Vawter, Appl. Phys. Lett. 63 (1993) 2457.
[17] H. Man, D.V. Forbes, J.J. Coleman, IEEE J. Quantum Electron. 3l (1995) 1994.
[18] C. Ji, M.H. Leary, J.M. Ballantyne, IEEE Photon Technol. Lett. 9 (1997) 1469.
[19] M.R. Krames, A.D. Minervini, N. Holonyak Jr., Appl. Phys. Lett. 67 (1995) 73.
[20] M.J. Grove, D.A. Hudson, P.S. Zory, R.J. Dallby, C.M. Harding, A. Rosenberg, J. Appl. Phys. 76 (1994) 587.
[21] C.C. Largent, C.H. Wu, M.J. Grove, P.S. Zory, D.P. Bour, IEEE LEOS '94 Conf. Proc. 1 (1994) 325.